How to cite: *Angew. Chem. Int. Ed.* **2021**, *60*, 9063–9070
International Edition: doi.org/10.1002/anie.202011848
German Edition: doi.org/10.1002/ange.202011848

Acenes

(Aza)Acenes Share the C2 Bridge with (Anti)Aromatic Macrocycles: Local vs. Global Delocalization Paths

*Krzysztof Bartkowski and Miłosz Pawlicki**

Dedicated to Professor Lechosław Latos-Grażyński on the occasion of his 70th birthday

Abstract: *A strong conjugation present in fused systems plays a crucial role in tuning of the properties that would be showing a dependence on the efficiency of π-electrons coupling. The π-cloud available in the final structure can be drastically influenced by a side- or a linear fusion of unsaturated and conjugated hydrocarbons. The linear welding of naphthalene/anthracene or quinoxaline/benzo[g]quinoxaline with triphyrin(2.1.1) gives structures where the competition between local and global delocalization is distinguished. The aromatic character observed in skeletons strongly depends on the oxidation state of the macrocyclic flanking and is either extended over the whole system or kept as a composition of local currents (diatropic and paratropic) of incorporated units. The hybrid systems show the properties derived from the π-conjugations that interlace one another but also show a significant independence of (aza)acene subunits reflected in the observed spectroscopic properties.*

Introduction

Unsaturated and strongly π-conjugated hydrocarbons are extensively explored as skeletons important for fundamental studies but also with a significant potential for practical applications. A cyclic construction of unsaturated hydrocarbons introduces the very fundamental phenomenon of aromaticity resulted from strongly delocalized π-electrons that give a diatropic current essential for observed properties and reactivity.[1] The gradual increase of the number of π-electrons allows a specific control of the spectroscopic response derived from a global conjugation.[2] Archetypal skeletons with a potential for increasing the π-conjugation by gradual fusion are acenes and azaacenes.[3] The extended conjugation of an (aza)acene is described as the equilibrium of several contributors where the Clar's sextet[4] shifts from one side to another significantly influencing the final outcome[3] but also having a substantial effect on the observed reactivity.[2] Beside the linear extension the π-cloud of acenes was efficiently modulated by merging with other π-extended molecules including strongly coupled macrocycles (e.g. porphyrinoids). The merging process of both structural motifs involves two modes of interaction: the linear extension on the C2 bridge and β-positions[5] and the edge-fashion (e.g. **1**).[6] Both types of interactions lead to different final outcome and substantially dissimilar contribution of local and global conjugations.

A modulation of delocalization in structures merging acenes and macrocycles can be also realized by a controlled linking of isolated motifs[7] simultaneously masking a specific behavior that after revealing via a fundamental process (e.g. redox)[8] strongly influence final response changing the observed π-delocalization path (e.g. **2**).[8,9] The redox process is one of the post-synthetic modification with a substantial influence on the conjugated π-cloud opening a path of switching between aromatic ($4n+2$ π-electrons)[2] and antiaromatic ($4n$ π-electrons) character[10] observed for porphyrinoids[11] but also (aza)acenes.[3] The modulation of aromatic character of both motifs needs using strong oxidizing or reducing agents what limits a possibility of exploring of the mutual influence of subunits incorporated in the hybrids. On the other hand a triphyrin(2.1.1) (e.g. **3**)[14] has been reported as the skeleton with the accessible aromatic/antiaromatic switching behavior.[15] The ethylene linker of triphyrins(2.1.1) (Figure 1) can be naturally used for welding with acene/heteroacene in the linear fashion. Potential hybrids are eventually formed with two well defined π-clouds and a potential for changing the oxidation state in one unit to form antiaromatic current that influence the π-cloud of (aza)acene.

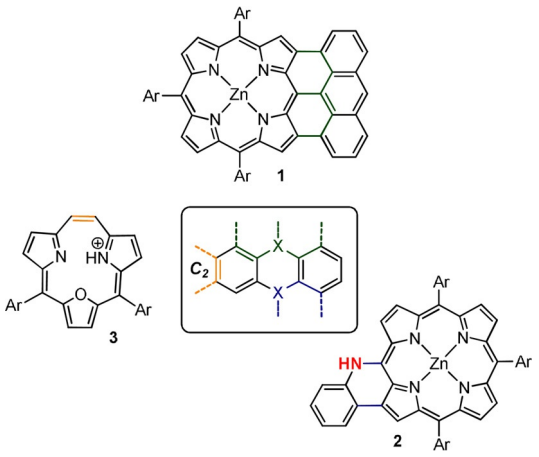

Figure 1. Acene-Macrocycle Hybrids.

[*] K. Bartkowski, Prof. M. Pawlicki
Department of Chemistry, University of Wrocław
F. Joliot-Curie 14, 50383 Wrocław (Poland)
Prof. M. Pawlicki
Faculty of Chemistry, Jagiellonian University
Gronostajowa 2, 30387 Kraków (Poland)
E-mail: pawlicki@chemia.uj.edu.pl
Homepage: http://mjplab.org
Supporting information and the ORCID identification number(s) for the author(s) of this article can be found under: https://doi.org/10.1002/anie.202011848.

Following these observations here we report on the modulation of the π-conjugation within hybrid skeletons built of acene/azaacene and macrocycle (Figure 2) and controlled by the aromatic-antiaromatic switch in the macrocyclic contributor. The observed optical response is dependent on the degree of planarization and results in competition between local and global delocalization with a substantial contribution of local effects documented in spectroscopy.

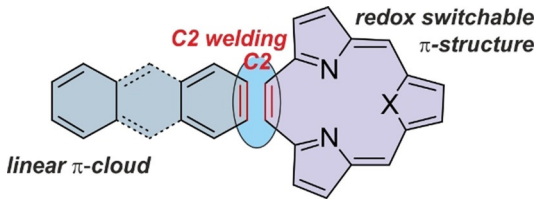

Figure 2. Acene-Switchable Macrocycle Edge Fused Hybrid.

Results and Discussion

The modulation of acene/azaacene π-cloud has been realized on the way of welding with a triphyrin(2.1.1) skeleton via a sequence of reactions requiring formation of proper derivatives of both acenes and azaacenes (Scheme 1). Acene derivatives were efficiently obtained on the way of Suzuki–Miyaura coupling starting from a commercially available dibromonaphthalene **4a** or obtained according to the previously reported procedure dibromoanthracene **4b**.[16] Both derivatives, subjected to catalytic reaction with *N*-BOC-pyrrole boronic acid followed by deprotection gave **6a** (58%) and **6b** (12%) (Scheme 1, *path a*). Both azaacenes requested an application of dipyrrole derivative **5** that after condensation (Scheme 1, *path b*) with *ortho*-phenylenediamine and 2,3-diaminonaphthalene gave **6c**[17] and **6d** with 67% and 96% yield, respectively. The subsequent condensation with 2,5-bis(3,5-di-*t*butylphenyl)-hydroxymethylfuran applied for **6a** and **6b** gave **7a** and **7b**, respectively (Scheme 1, *path c*), eventually isolated as cationic forms. Importantly both acene derivatives were obtained with good yields of 47% (**7a**) and 39% (**7b**) what shows a generality of applied approach but also effectiveness of condensation. The cationic character was indirectly confirmed by HRMS experiments where *m*/*z* peaks consistent with expected atomic composition (*m*/*z* observed 723.4219 expected 723.4309 for $C_{52}H_{55}N_2O$ (**7a**); *m*/*z* observed 773.4364 expected 773.4465 for $C_{56}H_{57}N_2O$ (**7b**)) were observed. The condensation of **6c**/**6d** required significantly different conditions with an excess of stronger acid (Scheme 1, *path d*). Even then the observed yields were substantially lower (6% (**7c**) and 5% (**7d**)) showing a dissimilar character of both linear systems of acene and azaacene. Similarly to the acene derivatives **7c** and **7d** were isolated as cations as documented in HRMS experiments where the *m*/*z* signals (observed 725.4219 expected 725.4214 for $C_{50}H_{53}N_4O$ (**7c**); observed 775.4382 expected 775.4370 for $C_{54}H_{55}N_4O$ (**7d**)) consistent with expected atomic composition were observed. In all four derivatives the unidentified counter ion was replaced with a tetrafluoroborane that increased the solubility and allowed a detailed spectroscopic analysis of all derivatives. All further experiments were performed on systems with tetrafluoroborate anion.

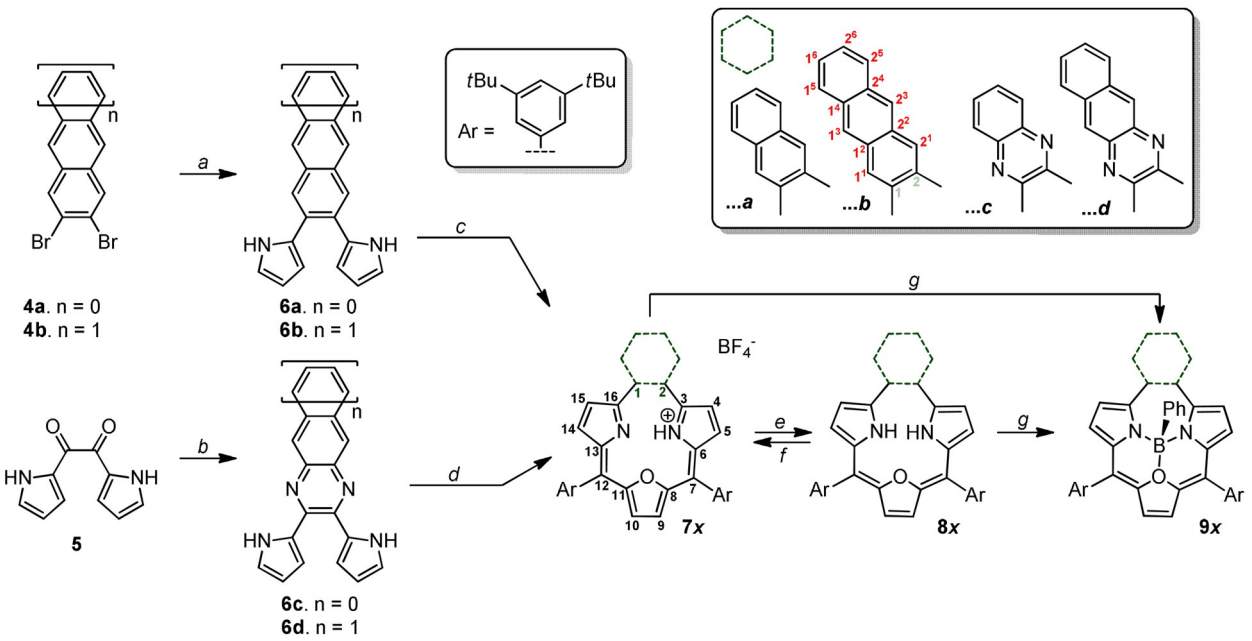

Scheme 1. Synthetic approach for formation of acene/azaacene-triphyrin(2.1.1) hybrids. *Conditions*: a) 1. (*N*-Boc-pyrrol-2-yl)boronic acid, K_2CO_3, Pd-$(PPh_3)_4$, THF, Toluene, H_2O, Aliquat 336, 95 °C, 24 h (**6a**)/18 h (**6b**). 2. $(CH_2OH)_2$ reflux, 1 h. b) *ortho*-Phenylenediamine (**6c**)/ Naphthalene-2,3-diamine (**6d**), AcOH, reflux, o/n; c) 1. 2,5-bis(3,5-di-*t*butylphenyl)hydroxymethylfuran, $BF_3{\cdot}Et_2O$, CH_2Cl_2, 4 h; 2. DDQ, 30 minutes, 3. $NaHCO_3$, HBF_4(aq). d) 1. 2,5-bis(3,5-di-*t*butylphenyl)hydroxymethylfuran, $HBF_4{*}Et_2O$, CH_2Cl_2, 48 h; 2. DDQ, 1 h, 3. $NaHCO_3$, HBF_4(aq). e) Zn/Hg, CD_2Cl_2; f) air or DDQ; g) $BPhCl_2$, Et_3N, Toluene, reflux 1 h (**9a**/**b**).

The extension of the π-cloud in conjugated systems significantly influence the UV/Vis absorption as documented for PAHs (e.g. (aza)acenes)[3] or macrocycles[5–8] including triphyrins(2.1.1).[14,15] The UV/Vis spectra of **7a** and **7c** (Figure 3A) with intense Soret bands ($\lambda = 434$ nm and $\lambda = 421$ nm, respectively) accompanied by a set of Q-bands with the most red-shifted band at $\lambda = 662$ nm (**7a**) and $\lambda = 588$ nm (**7c**) (Figure 3A) show the picture consistent with the significant contribution of globally extended delocalization involving both subunits of the hybrid systems and characteristic for aromatic porphyrinoids.[13,15] Substantially different optical properties were recorded for **7b** and **7d** with the sharp absorbance at $\lambda = 458$ nm and $\lambda = 452$ nm, respectively and the Q-region tailing to $\lambda = 850$ nm (**7b**) and $\lambda = 800$ nm (**7d**).

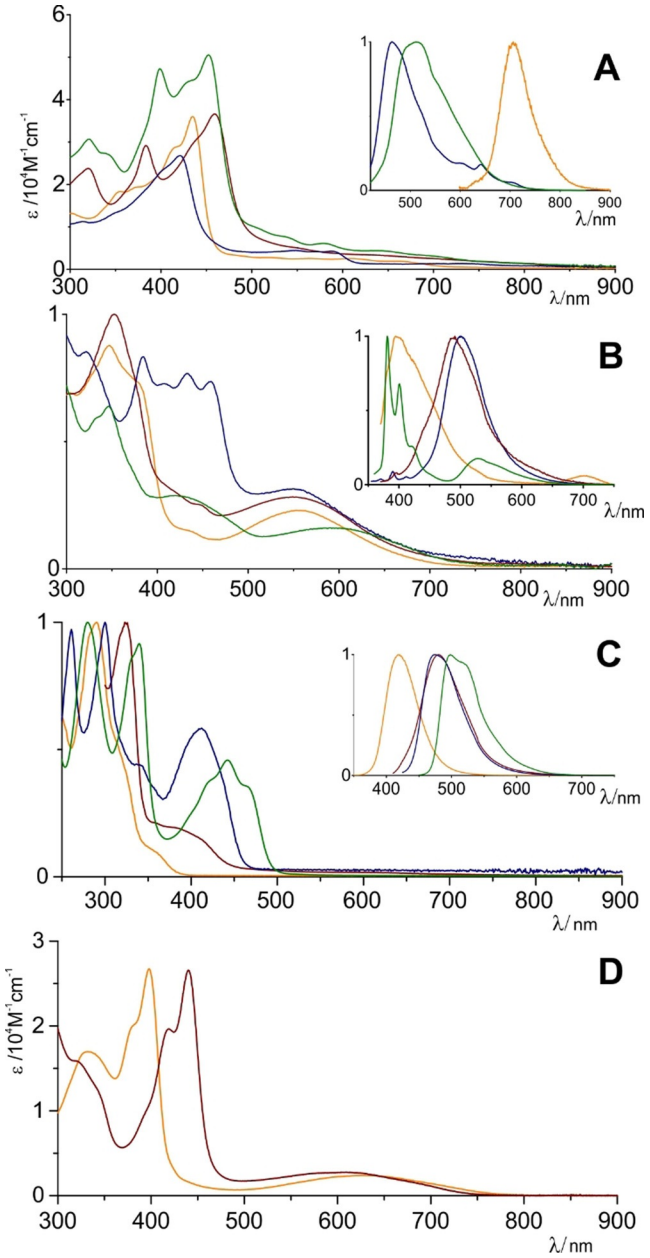

Figure 3. Absorbance and emission spectra of **7x** (A, CH_2Cl_2), **8x** (B, CH_2Cl_2), **6x** (C, CH_2Cl_2) and **9x** (D, CH_2Cl_2). All spectra measured at 298 K. Colour Scheme applied: orange (naphthalene, **Ya**), wine (anthracene, **Yb**), blue (quinoxaline, **Yc**), green (benzo[g]quinoxaline, **Yd**).

It suggests more complex behavior of both hybrids **7b**/**7d** and a potential contribution of local effects. A mutual interaction of both subunits was deeply modified in the redox switched structures **8x** obtained quantitatively with a zinc amalgam (Scheme 1, *path e*). The presence of paratropic current modulates the global delocalisation what finds a reflection in the UV/Vis spectra.[15,18] The four hybrids (**8a–d**) show significantly different UV/Vis spectra supporting a substantial modification of available π-electrons and consistent with their 4*n* number (Figure 3B). Nevertheless, the observed complex shapes show dissimilar pattern to other 4*n* systems based on triphyrin(2.1.1),[15] where the intense Soret band is accompanied by bathochromically shifted absorption with a small oscillator strength.[18] The reduced acene derivatives **8a**/**8b** were efficiently entrapped as boron(III) complexes **9a**/**9b** (Scheme 1, *path g*) which prevents from back oxidation to **7** which occurs efficiently as documented in time-evolved experiments monitored with UV/Vis (Scheme 1, *path f*, Figure S57-60). **9a** and **9b** showed nicely marked molecular peaks in HRMS (*m*/*z* observed 841.4863 expected 841.4909 for $C_{59}H_{62}BN_2O_2$ (**9a**), *m*/*z* observed 891.4997 expected 891.5066 for $C_{63}H_{64}BN_2O_2$ (**9b**)) consistent with the expected atom composition confirmed also by the isotopic pattern (Figure S49,50). We were unable to obtain boron(III) complexes for **7c**/**7d**. The oxidation state of macrocyclic part in **8** and **9** is similar but the pattern of observed spectra shows substantial differences (Figure 3B,D) suggesting a behaviour dependent on expected planarity. The reduced forms of macrocycles entrapped in boron(III) complexes **9x** showed a significantly different absorbance while comparing to **7x** (Figure 3D) with a sharp band in the $\lambda =$ 350–470 nm region and the broad absorption at $\lambda = 500$–750 nm with the pattern observed for partially antiaromatic compounds.[15,18]

The crucial information about the behaviour and mutual influence of both subunits was derived from the observed emission spectra. As expected for a dominating contribution of globally π-extended delocalisation in **7a** a single maximum at $\lambda_{em} = 708$ nm and Stokes shift of ≈45 nm, characteristic for triphyrin derivatives was recorded.[14,15] In the same experiment **7c** and **7d** showed emissions shifted hipsochromically ($\lambda_{em} = 450$ and $\lambda_{em} = 500$ nm, respectively (Figure 3A, inset, blue and green)) while **7b** has been documented as non-emissive. The emission wavelength of **7a** supported by the excitation experiment performed at the λ_{em} (Figure S61) suggest that the red shifted band of fluorescence is associated with the global delocalisation. A surprising emission recorded for **7c** and **7d** at the shorter wavelengths and comparable to those recorded for **6x** (Figure 3C) suggests a substantial contribution of local effects assigned to (aza)acene incorporated to final structure in addition the excitation spectra recorded show the pattern with maxima recorded for **6c**/**6d**. The local effect of conjugation resulting in the shortwave emission overlapping with the absorption spectrum has been recorded for complex structures for example in corrole derivatives.[19] The local delocalisation effects has been even more marked for the reduced structures **8x** that, in contrast to

typical $4n$ π-electrons systems,[18] showed emission. The observed fluorescence (Figure 3B, inset, $\lambda_{em} = 430$ nm (**8a**), $\lambda_{em} = 494$ nm (**8b**), $\lambda_{em} = 482$ nm (**8c**)) was recorded in the spectral region observed previously for dipyrrolic derivatives **6x** (Figure 3C, inset). It suggests an independent character of (aza)acene(s) in the final molecule as the excitation spectra of **8a–c** (Figure S72–76) fairly reproduce those observed for **6x**. The emission for **8d** was observed at $\lambda_{em} = 381$ nm what is substantially blue shifted even while compering to **6d** ($\lambda_{em} \approx 520$ nm) suggesting even deeper isolation of delocalization paths of benzo[*g*]quinoxaline and reduced triphyrin(2.1.1). The both boron(III) complexes **9a** and **9b** showed lack of emission consistently with the predicted more efficient paratropic current.[15,18]

Both types of the currents—diatropic or paratropic—can be diagnosed following the magnetic criterion of aromaticity based on ^{1}H NMR spectra.[20] The series of oxidized derivatives **7x** showed the ^{1}H chemical shifts of the β-lines of all heterocyclic subunits located in the region of 9.0–7.5 ppm consistent with a noticeable contribution of global delocalisation (Figure 4B **7a**, Figures S45–47)[20] but also underlining the structural modifications. The most significant difference can be observed for resonances assigned to positions 4,15 significantly downfield shifted in azaacene derivatives ($\delta =$ 9.10 ppm **7c** and $\delta = 8.96$ ppm **7d**) while comparing to acene hybrids ($\delta = 8.48$ ppm **7a**, $\delta = 8.30$ ppm **7b**) and caused by the proximity of nitrogens.[12f] In contrast to typical behavior in aromatic macrocycles the inner hydrogens of **7a–d** showed a substantial downfield shift ($\delta = 17.01$ ppm (**7a**); $\delta =$ 18.54 ppm (**7b**); $\delta = 15.62$ ppm (**7c**); $\delta = 17.08$ ppm (**7d**)) consistent with a strong hydrogen bond documented in crystal structure(s)[21] that competes with the diatropic current influence.[22] The two-electron reduced derivatives that showed a significant disturbance of the global delocalisation what has been also reflected in ^{1}H chemical shifts range for the β-lines (Figure 4C **8a**, Figures S45-47) recorded between $\delta = 5.2$–6.2 ppm and consistent with a contribution of local effects.[20] The NH resonances were shifted upfield while compering to **7x** ($\delta = 12.51$ ppm (**8a**); $\delta = 12.06$ ppm (**8b**); $\delta = 13.54$ ppm (**8c**); $\delta = 12.70$ ppm (**8d**)) showing a significant influence of N-H-N hydrogen bond unavailable for non-planar geometry of **8x**. Boron(III) complexes shifts β-lines upfield (**9a** $\delta = 6.37$ ppm (4,15), $\delta = 5.99$ ppm (5,14), $\delta =$ 5.74 ppm (9,10) (Figure 4D), and for **9b** $\delta = 6.61$ ppm (4,15), $\delta = 6.15$ ppm (5,14), $\delta = 5.94$ ppm (9,10)), locating those systems on the border between non-aromatic and antiaromatic structures.[15,20] The chemical shifts of the axial aryl group attached to the central boron inside the macrocycle are sensitive probes for assessing the aromatic character of the macrocycle.[15,23] The downfield shifted resonances of the axial phenyl group (Figure 4D; **9a** $\delta = 8.22$ ppm *ortho*, $\delta =$ 7.48 ppm *meta*, $\delta = 7.42$ ppm *para*; **9b** $\delta = 7.93$ ppm *ortho*, $\delta =$ 7.39 ppm *meta*, $\delta = 7.34$ ppm *para*) confirm that the macrocycle is slightly antiaromatic.[15,20,24]

The presence of diatropic or paratropic current was expected to substantially affect the fused (aza)acene resonances crucial for assessing the contribution of global or local delocalisation(s). Actually the range of chemical shifts (δ) is an intuitive tool helpful in assessing the contribution of a global and local diatropic π-expansion that de-shields the perimeter lines shifting them down-field.[7,8,19] A typical behavior of the paratropic current is the up-field relocation of the margin resonances.[15,18,20] The lack of global effect either diatropic or paratropic will leave the influence of local conjugation characteristic for unsaturated carbocycles or heterocycles. Thus, it is expected that changes in the character of analyzed molecules and being a consequence of switching from diatropic to paratropic current will significantly influence the observed δ range. The observed chemical shifts of naphthalene subunit in **7a** ($\delta = 9.94$ ppm (1^1,2^1), $\delta = 8.59$ ppm (1^3,2^3), $\delta = 8.10$ ppm (1^4,2^4)) show a noticeable down-field shift while comparing to **6a** ($\delta = 7.92$ ppm (1^1,2^1), $\delta =$ 7.79 ppm (1^3,2^3), $\delta = 7.44$ ppm (1^4,2^4)) consistently with efficient global delocalization and significant contribution of 22π electrons path (Figure 4A,B, *green arrow*). The two-electron reduction and formation of **8a** shifts the discussed resonances up-field ($\delta = 7.72$ ppm (1^1,2^1), $\delta = 7.60$ ppm (1^3,2^3), $\delta =$ 7.32 ppm (1^4,2^4)) to positions comparable to **6a**, consistently with breaking the global extension of delocalization (Figure 4C) and stabilizing the local effects. The correlation of the chemical shift with the oxidation state is also observed for boron(III) complexes ($\delta = 7.23$ ppm (1^1,2^1), $\delta = 7.37$ ppm (1^3,2^3), $\delta = 7.14$ ppm (1^4,2^4) **9a**) comparable with **6a** (Figure 4D) and consistent with the lack of global effect and stabilization of both characters (diatropic and paratropic). Similar trend was recorded for quinoxaline derivatives **7c** (Figure S46). The longer (aza)acenes of **7b** and **7d** show the perimeter protons downfield shifted by $\Delta \approx 1.1$–1.5 ppm while comparing with **6b** and **6d** supporting a less efficient global

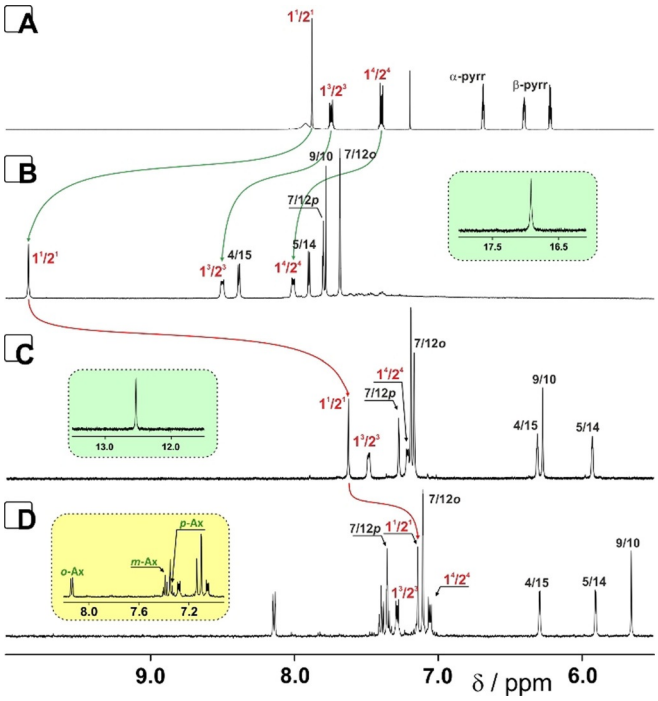

Figure 4. ^{1}H NMR spectra (600 MHz, 300 K) for **6a** (A, $CDCl_3$), **7a** (B, CD_2Cl_2), **8a** (C, $CDCl_3$) and **9a** (D, CD_2Cl_2). A shift of $1^1/2^1$ naphthalene resonances marked with green and red arrows shows a change in chemical shifts and modulation of the observed currents.

delocalization concluded from the electronic spectra (Figure S45 and S47). The reduced skeletons of **8b–d** showed similar trends presenting a good correlation of chemical shifts assigned to (aza)acenes subunits with linear substrates **6b**, **6c**, **6d** consistent with a lack of global effect deduced from electronic properties (see SI). It also proves that the two-electron reduction and conversion from **7x** to **8x** blocks the macrocyclic delocalization and leaves an (aza)acene to operate as an independent subunit.

Changes in delocalization paths can be also derived from structural parameters (bond lengths or angles) available from crystal structures. As observed in the X-Ray structure of **7a** (Figure 5A) the main motif of the final molecule is planar with the hydrogen entrapped inside of the cavity.[14,15,21] The NON cavity creates an environment with the distances (N-N 2.526 Å, N-O 2.521 Å) consistent with strong three-center hydrogen entrapment within the confined cavity of triphyrinic flanking.[15] Importantly the formation of linear extension of acene π-cloud with a macrocyclic ending does not change the planarity of acene and in addition the whole molecule creates strongly planarized conformation. The X-ray analyses of **7a**/**9a** couple (Figure 5A,B) showed a noticeable trend in changing of the C(1)-C(2) bond length as the most crucial for discussing global vs. local effects competition. The C(1)-C(2) bond lengths in **7a** (1.485 Å) is significantly longer while comparing to **6a** (1.431 Å, Figure 5A, inset) consistent with a contribution of global delocalization in strongly extended π-cloud of acene-triphyrin hybrid. The C(1)-C(2) bond length in **9a** is shorted (1.439 Å) suggesting a presence of two local effects as observed in spectroscopy. The crystal structure of **9b** (Figure 5C) confirmed a better interaction between acene and macrocyclic motif increasing the efficiency of π-π overlap significantly influencing the optical response.[19] Both complexes showed a different packing dependent on the type of the employed acene. Naphthalene derivative **9a** showed a head-to-tail organization (Figure 5B, inset) with naphthalene edge pointing to the furan subunit while in **9b** a head-to-head of anthracenes is observed in addition stabilized by the π-π interaction (Figure 5C, inset). Thus, all experimental evidences show a difference in observed quality of conjugation depending on the type of involved (aza)acene and a significant contribution of global (**7a**/**7c**) or local (**7b**/**7d**) delocalization(s). The local contributors are significantly marked in two electron reduced structures **8x** and confirmed by the recorded emission(s) at λ_{max} comparable to **6x**.[7,8,19,25] The lack of local of emission in boron(III) complexes **9a**/**9b** is consistent with a contribution of paratropic current.

To get a deeper insight into the observed behaviour and modulable delocalization paths we conducted theoretical analyses for all presented motifs with the B3LYP functional and at the 6-31G(d,p) level of theory. The optimized models were compared with available crystal structures showing a good correlation of geometries crucial for reliable of analysis conducted on conjugated macrocycles.[14,15,20] The theoretical models of **7x** show a significant planarity (Figure S77–80) while the geometries of reduced forms (**8x**) are strongly disturbed from planarity because of steric repulsion of two NH groups present in the limited space of macrocycle cavity (see SI, Figure S77–80). It is consistent with the observed spectroscopic behavior and strongly disturbed global delocalization. Similarly to the crystal structure of **9a**/**9b** all geometries optimized for boron(III) complexes showed a substantial planarity responsible for efficient π-π overlap that supports a presence of a paratropic current. The GIAO predictions of the ^{1}H NMR chemical shifts reproduced the recorded patterns for all analyzed structures (see the Supporting Information, Table S3/S4). The fully optimized structures of **7x**, **8x**, and **9x** have been used for NICS(1) (nucleus independent chemical shift)[27] and AICD (anisotropy induced current density)[28] analyses (Figure 6). It can be easily noticed that the fusion of 10π electrons of naphthalene or quinoxaline in **7a** and **7c**, respectively opens a global 22π delocalization as observed in AICD profiles (Figure 6, A1/B1) efficiently switching off the local effects of separated units. In contrast to that the longer (aza)acenes—anthracene and benzo[*g*]quinoxaline in **7b** and **7d**, respectively—show the competition between two local effects (Figure 6, C1/D1) keeping the 14π delocalization of (aza)acene and diminished global contribution of potential 26π path. The NICS(1) calculated within macrocylic motifs (points *a* and *e*) show noticeably negative values for **7a** and **7c** that are significantly lowering for **7b** and **7d** (Figure 6) consistently with recorded spectroscopic behaviour and substantially different global aromatic character. The (aza)acenes subunits incorporated in all oxidized derivatives were characterized as strongly aromatic based on observed NICS-

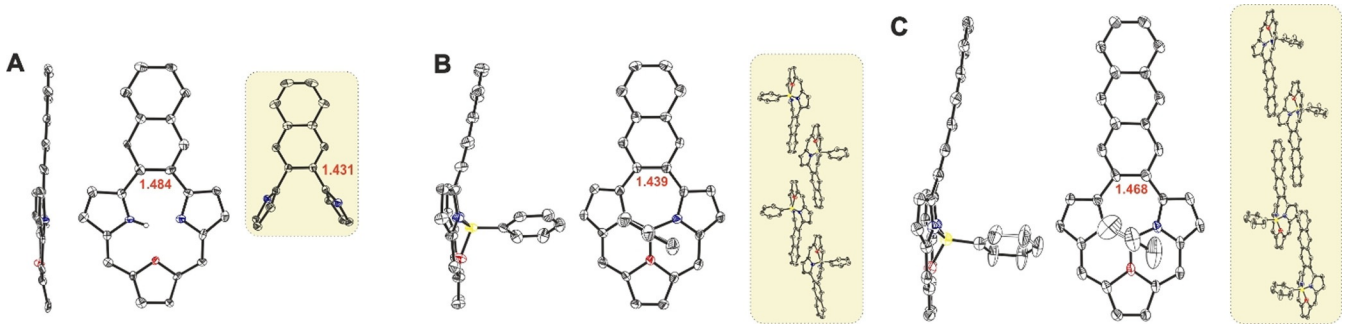

Figure 5. Crystal structures for **7a** (A) **9a** (B) and **9b** (C). Thermal ellipsoids present 50% (A,B) and 30% (C) probability. Inset in trace A presents the crystal structure for linear naphthalene-pyrrole structure (50% thermal ellipsoids). In traces B and C the mutual interaction between acene-macrocycle hybrids are presented showing a π-π interaction. *Meso*-aryls are omitted for clarity.[26]

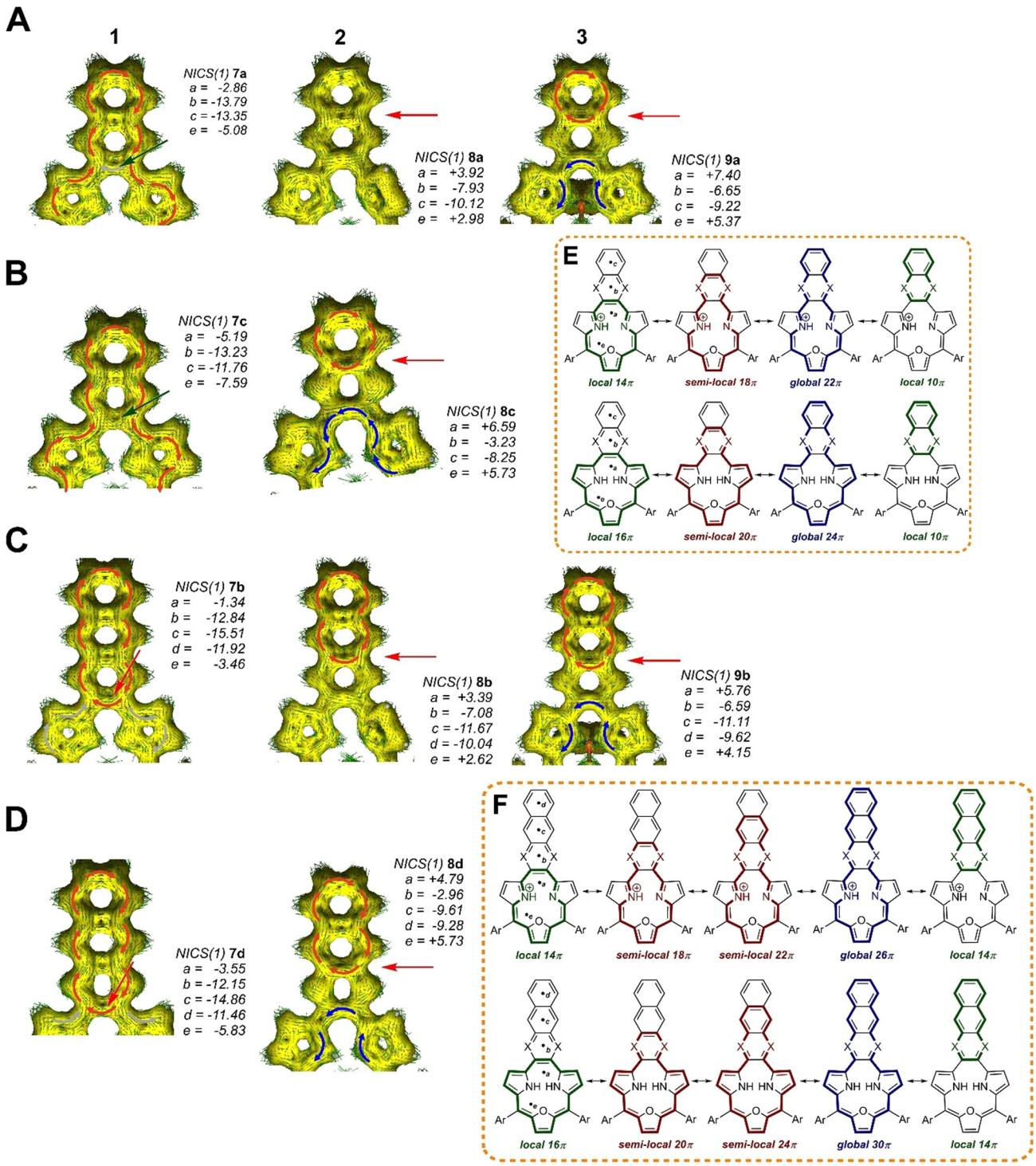

Figure 6. AICD profiles for analysed derivatives (isovalue 0.035) (A-D/1–3) and NICS(1) values calculated in points a–e. Traces E and F present possible resonance contributions of the oxidized and reduced variants of (aza)acene-macrocycle hybrids. Red arrows show clockwise current characteristic for aromatic systems and blue arrows show anticlockwise current typical for paratropic delocalization in analysed structures.

(1) values (Figure 6, points *b*,*c*,*d*). The AICD profiles obtained for the two-electron reduced oxidation systems **8x** showed a presence of paratropic current in the macrocyclic motif significantly influencing the diatropic current within PAH and opening an opportunity for having a contribution of local effects of 6π (**8a**/**8c**) and 10π (**8b**/**8d**) (Figure 6, A2/B2/C2/D2). It suggests a potential for stabilization of two opposite currents aromatic in a carbocycle and antiaromatic in a macrocyclic part. The NICS(1) values obtained for **8x** series with noticeably positive values in macrocyclic part (Figure 6, points a and e) consistently support separation of delocalization paths of a weak paratropic current in macro-

cyclic part and a diatropic flow in an acene unit. The significantly lowered NICS(1) values observed at point *b* especially for **8c** and **8d** with strongly negative values of NICS(1) recorded for the 6π and 10π fused system (points *c*, *d*), respectively consistently support substantial contribution of local effects. The drastic change of spectroscopic behavior assigned to observed co-planarity of both components in boron(III) complexes **9a**/**9b** finds further confirmation in theoretical analysis (Figure 6, A3 and C3). The AICD profiles and NICS(1) values obtained for both boron(III) complexes show more efficient paratropic current in macrocyclic motif followed by further separation of 6π (**9a**) and 10π (**9b**) aromatic paths in acenes.

Conclusion

We have carefully planned the synthesis of hybrid material opening a possibility for modulation of acene/azaacene properties by merging with a redox switchable macrocycle of triphyrin(2.1.1). Both components share the C2 bridge that allows a transmission of global aromatic delocalization over the whole molecule observed for $4n+2$ π-electrons entrapped in the system. Depending on the (aza)acene a 22π delocalization (naphthalene/quinoxaline) and 26π (anthracene/benzo[*g*] quinoxaline) global path is potentially available. The two electron reduction of the redox sensitive fragment of the hybrid systems introduces a $4n$ π-electrons motif and converts the globally delocalized structure to the non-planar system where the local effect of (aza)acene deeply modifies observed properties as documented spectroscopically. The planarization of $4n$ π-electrons system via a boron(III) insertion increases an influence of the paratropic current of macrocyclic part switching off the behavior recorded for ruffled skeleton(s). Importantly a significant difference in efficiency of observed effects can be assigned to different linker between acene and macrocycle. Considerably more efficient influence can be assigned to nitrogen linkers in both types of skeletons—oxidized and reduced—where more efficient global effects of diatropic current and better separation of two opposite delocalization was observed for **7c**/**8c** and **7d**/**8d**. Thus, the hybrid material constructed of (aza)acene and a modifiable macrocycle can be treated as a skeleton where several effects are interlacing one another masking the local behavior while forming a planar structure of fully delocalized and aromatic 22π/26π system. The redox switch of the (aza)acene side-decoration strongly influences the final system with the paratropic current of boron(III) complex switching off the fluorescence. Significantly the two-electron reduction entrapping strongly ruffled geometry revels the local effects as documented in the fluorescence behavior and confirmed with the theoretical analysis.

Acknowledgements

Financial support from the National Science Centre, Poland (2015/17/B/ST5/01437) is kindly acknowledged. The Wrocław Supercomputer Centre (KDM WCSS) is kindly acknowledged for sharing computation resources necessary for DFT calculations.

Conflict of interest

The authors declare no conflict of interest.

Keywords: acene · antiaromaticity · aromaticity · azaacene · triphyrin

[1] a) R. Gleiter, G. Haberhauer, *Aromaticity and Other Conjugation Effects*, Wiley-VCH, Weinheim, **2012**; b) T. M. Krygowski, M. K. Cyrański, Z. Czarnocki, G. Häfelinger, A. R. Katritzky, *Tetrahedron* **2000**, *56*, 1783 – 1796.
[2] J. A. N. F. Gomes, R. B. Mallion, *Chem. Rev.* **2001**, *101*, 1349 – 1383.
[3] a) R. Dorel, A. M. Echavarren, *Eur. J. Org. Chem.* **2017**, 14 – 24; b) A. Bedi, O. Gidron, *Acc. Chem. Res.* **2019**, *52*, 2482 – 2490; c) U. H. F. Bunz, *Acc. Chem. Res.* **2015**, *48*, 1676 – 1686; d) A. Mateo-Alonso, *Chem. Soc. Rev.* **2014**, *43*, 6311 – 6324; e) J. E. Anthony, *Angew. Chem. Int. Ed.* **2008**, *47*, 452 – 483; *Angew. Chem.* **2008**, *120*, 460 – 492; f) U. H. F. Bunz, J. Freudenberg, *Acc. Chem. Res.* **2019**, *52*, 1575 – 1587; g) X. Shi, C. Chi, *Chem. Rec.* **2016**, *16*, 1690 – 1700.
[4] a) K. J. Thorley, J. E. Anthony, *Isr. J. Chem.* **2014**, *54*, 642 – 649; b) C. H. Suresh, S. R. Gadre, *J. Org. Chem.* **1999**, *64*, 2505 – 2512; c) M. Solà, *Front. Chem.* **2013**, *1*, 22; d) M. Bendikov, H. M. Duong, K. Starkey, K. N. Houk, E. A. Carter, F. Wudl, *J. Am. Chem. Soc.* **2004**, *126*, 7416 – 7417.
[5] T. Tanaka, A. Osuka, *Chem. Soc. Rev.* **2015**, *44*, 943 – 969.
[6] a) S. Richeter, C. Jeandon, J.-P. Gisselbrecht, R. Ruppert, H. J. Callot, *J. Am. Chem. Soc.* **2002**, *124*, 6168 – 6179; b) S. Fox, R. W. Boyle, *Chem. Commun.* **2004**, 1322 – 1323; c) D.-M. Shen, C. Liu, Q.-Y. Chen, *Chem. Commun.* **2005**, 4982 – 4984; d) E. Hao, F. R. Fronczek, M. G. H. Vicente, *J. Org. Chem.* **2006**, *71*, 1233 – 1236; e) H. S. Gill, M. Marmjanz, J. Santamaria, I. Finger, M. J. Scott, *Angew. Chem. Int. Ed.* **2004**, *43*, 485 – 490; *Angew. Chem.* **2004**, *116*, 491 – 496; f) A. N. Cammidge, P. J. Scaife, G. Berber, D. L. Hughes, *Org. Lett.* **2005**, *7*, 3413 – 3416; g) M. Tanaka, S. Hayashi, S. Eu, T. Umeyama, Y. Matano, H. Imahori, *Chem. Commun.* **2007**, 2069 – 2071; h) O. Yamane, K. Sugiura, H. Miyasaka, K. Nakamura, T. Fujimoto, K. Nakamura, T. Kaneda, Y. Sakata, M. Yamashita, *Chem. Lett.* **2004**, *33*, 40 – 41; i) K. Kurotobi, K. S. Kim, S. B. Noh, D. Kim, A. Osuka, *Angew. Chem. Int. Ed.* **2006**, *45*, 3944 – 3947; *Angew. Chem.* **2006**, *118*, 4048 – 4051; j) N. K. S. Davis, M. Pawlicki, H. L. Anderson, *Org. Lett.* **2008**, *10*, 3945 – 3947.
[7] M. Pawlicki, *Synlett* **2020**, *31*, 1 – 6.
[8] a) W. Stawski, K. Hurej, J. Skonieczny, M. Pawlicki, *Angew. Chem. Int. Ed.* **2019**, *58*, 10946 – 10950; *Angew. Chem.* **2019**, *131*, 11062 – 11066; b) M. Pawlicki, K. Hurej, K. Kwiecińska, L. Szterenberg, L. Latos-Grażyński, *Chem. Commun.* **2015**, *51*, 11362 – 11365; c) K. Hurej, W. Stawski, L. Latos-Grażyński, M. Pawlicki, *Chem. Asian J.* **2016**, *11*, 3329 – 3333.
[9] M. Farinone, J. Cybińska, M. Pawlicki, *Org. Chem. Front.* **2019**, *6*, 2825 – 2832.
[10] R. Breslow, *Acc. Chem. Res.* **1973**, *6*, 393 – 398.
[11] a) M. D. Peeks, T. D. W. Claridge, H. L. Anderson, *Nature* **2017**, *541*, 200 – 203; b) M. D. Peeks, M. Jirasek, T. D. W. Claridge, H. L. Anderson, *Angew. Chem. Int. Ed.* **2019**, *58*, 15717 – 15720; *Angew. Chem.* **2019**, *131*, 15864 – 15867; c) Y. Ni, T. Y. Gopalakrishna, H. Phan, T. Kim, T. S. Herng, Y. Han, T. Tao, J. Ding, D. Kim, J. Wu, *Nat. Chem.* **2020**, *12*, 242 – 248; d) Z. Li, T. Y.

Gopalakrishna, Y. Han, Y. Gu, L. Yuan, W. Zeng, D. Casanova, J. Wu, *J. Am. Chem. Soc.* **2019**, *141*, 16266 – 16270; e) L. Ren, T. Y. Gopalakrishna, I.-H. Park, Y. Han, J. Wu, *Angew. Chem. Int. Ed.* **2020**, *59*, 2230 – 2234; *Angew. Chem.* **2020**, *132*, 2250 – 2254.

[12] a) M. J. Crossley, P. L. Burn, *J. Chem. Soc. Chem. Commun.* **1987**, 39 – 40; b) M. J. Crossley, L. G. King, *J. Chem. Soc. Chem. Commun.* **1984**, 920 – 922; c) T. Khoury, M. J. Crossley, *Chem. Commun.* **2007**, 4851 – 4853; d) M. J. Crossley, P. L. Burn, S. S. Chew, F. B. Cuttance, I. A. Newsom, *J. Chem. Soc. Chem. Commun.* **1991**, 1564 – 1566; e) K. Kise, A. Osuka, *Chem. Eur. J.* **2019**, *25*, 15493 – 15497; f) D. Kuzuhara, M. Sakaguchi, W. Furukawa, T. Okabe, N. Aratani, H. Yamada, *Molecules* **2017**, *22*, 908; g) B. Szyszko, D. Dróżdż, A. Sarwa, S. G. Mucha, A. Białońska, M. J. Białek, K. Matczyszyn, L. Latos-Grażyński, *Org. Chem. Front.* **2020**, *7*, 1430 – 1436.

[13] a) H. Uoyama, K. S. Kim, K. Kuroki, J.-Y. Shin, T. Nagata, T. Okujima, H. Yamada, N. Ono, D. Kim, H. Uno, *Chem. Eur. J.* **2010**, *16*, 4063 – 4074; b) J. Nakamura, T. Okujima, Y. Tomimori, N. Komobuchi, H. Yamada, H. Uno, N. Ono, *Heterocycles* **2010**, *80*, 1165 – 1175; c) M. Pawlicki, M. Morisue, N. K. S. Davis, D. G. McLean, J. H. Haley, E. Beuerman, M. Drobizhev, A. Rebane, A. L. Thompson, S. I. Pascu, G. Accorsi, N. Armaroli, H. L. Anderson, *Chem. Sci.* **2012**, *3*, 1541 – 1547; d) K. Oohora, A. Ogawa, T. Fukuda, A. Onoda, J. Hasegawa, T. Hayashi, *Angew. Chem. Int. Ed.* **2015**, *54*, 6227 – 6230; *Angew. Chem.* **2015**, *127*, 6325 – 6328.

[14] a) Z.-L. Xue, Z. Shen, J. Mack, D. Kuzuhara, H. Yamada, T. Okujima, N. Ono, X.-Z. You, N. Kobayashi, *J. Am. Chem. Soc.* **2008**, *130*, 16478 – 16479; b) K. S. Anju, S. Ramakrishnan, A. Srinivasan, *Org. Lett.* **2011**, *13*, 2498 – 2501; c) D. Kuzuhara, Y. Sakakibara, S. Mori, T. Okujima, H. Uno, H. Yamada, *Angew. Chem. Int. Ed.* **2013**, *52*, 3360 – 3363; *Angew. Chem.* **2013**, *125*, 3444 – 3447; d) D. Kuzuhara, S. Kawatsu, W. Furukawa, H. Hayashi, N. Aratani, H. Yamada, *Eur. J. Org. Chem.* **2018**, 2122 – 2129; e) A. Kumar, K. Thorat, M. Ravikanth, *Org. Lett.* **2018**, *20*, 4871 – 4874; f) K. N. Panda, K. G. Thorat, M. Ravikanth, *J. Org. Chem.* **2018**, *83*, 12945 – 12950; g) D. Kuzuhara, H. Yamada, *Heterocycles* **2013**, *87*, 1209 – 1240.

[15] a) M. Pawlicki, K. Hurej, L. Szterenberg, L. Latos-Grażyński, *Angew. Chem. Int. Ed.* **2014**, *53*, 2992 – 2996; *Angew. Chem.* **2014**, *126*, 3036 – 3040; b) M. Pawlicki, M. Garbicz, L. Szterenberg, L. Latos-Grażyński, *Angew. Chem. Int. Ed.* **2015**, *54*, 1906 – 1909; *Angew. Chem.* **2015**, *127*, 1926 – 1929; c) K. Bartkowski, M. Dimitrova, P. J. Chmielewski, D. Sundholm, M. Pawlicki, *Chem. Eur. J.* **2019**, *25*, 15477 – 15482.

[16] a) D. Bailey, V. E. Williams, *Tetrahedron Lett.* **2004**, *45*, 2511; b) T. Iwanaga, N. Asano, H. Yamada, S. Toyota, *Tetrahedron Lett.* **2019**, *60*, 1113 – 1116.

[17] C. B. Black, B. Andrioletti, A. C. Try, C. Ruiperez, J. L. Sessler, *J. Am. Chem. Soc.* **1999**, *121*, 10438 – 10439.

[18] S. Cho, Z. S. Yoon, K. S. Kim, M.-C. Yoon, D.-G. Cho, J. L. Sessler, D. Kim, *J. Phys. Chem. Lett.* **2010**, *1*, 895 – 900.

[19] B. Basumatary, R. V. R. Reddy, J. Sankar, *Angew. Chem. Int. Ed.* **2018**, *57*, 5052 – 5056; *Angew. Chem.* **2018**, *130*, 5146 – 5150.

[20] M. Pawlicki, L. Latos-Grażyński, *Chem. Asian J.* **2015**, *10*, 1438 – 1451.

[21] a) M. Pawlicki, L. Szterenberg, L. Latos-Grażyński, *J. Org. Chem.* **2002**, *67*, 5644 – 5653; b) J. Klajn, W. Stawski, J. Cybińska, P. J. Chmielewski, M. Pawlicki, *Chem. Commun.* **2019**, *55*, 4558 – 4561.

[22] a) I. C. Calder, F. Sondheimer, *Chem. Commun.* **1966**, 904 – 905; b) E. L. Spitler, C. A. Johnson II, M. M. Haley, *Chem. Rev.* **2006**, *106*, 5344 – 5386; c) C. D. Stevenson, T. L. Kurth, *J. Am. Chem. Soc.* **2000**, *122*, 722 – 723.

[23] a) J. A. Cissell, T. P. Vaid, G. P. A. Yap, *J. Am. Chem. Soc.* **2007**, *129*, 7841 – 7847; b) J. A. Cissell, T. P. Vaid, A. G. DiPasquale, A. L. Rheingold, *Inorg. Chem.* **2007**, *46*, 7713 – 7715; c) A. Młodzianowska, L. Latos-Grażyński, L. Szterenberg, M. Stępień, *Inorg. Chem.* **2007**, *46*, 6950 – 6957; d) A. Idec, M. Pawlicki, L. Latos-Grażyński, *Inorg. Chem.* **2017**, *56*, 10337 – 10352; e) M. Pawlicki, A. Kędzia, D. Bykowski, L. Latos-Grażyński, *Chem. Eur. J.* **2014**, *20*, 17500 – 17506.

[24] T. Kakui, S. Sugawara, Y. Hirata, S. Kojima, Y. Yamamoto, *Chem. Eur. J.* **2011**, *17*, 7768 – 7771.

[25] a) C. K. Frederickson, B. D. Rose, M. M. Haley, *Acc. Chem. Res.* **2017**, *50*, 977 – 987; b) J. L. Marshall, K. Uchida, C. K. Frederockson, C. Schutt, A. M. Zeidell, K. P. Goetz, T. W. Finn, K. Jarolimek, L. N. Zakharov, C. Risko, R. Herges, O. D. Jurchescu, M. M. Haley, *Chem. Sci.* **2016**, *7*, 5547 – 5558; c) R. E. Messersmith, S. Yadav, M. A. Siegler, H. Ottosson, J. D. Tovar, *J. Org. Chem.* **2017**, *82*, 13440 – 13448.

[26] Deposition Numbers 2020640 (for **7a**) 2020639 (for **9a**), 2020638 (for **6**), 2020637 (for **9b**) contain the supplementary crystallographic data for this paper. These data are provided free of charge by the joint Cambridge Crystallographic Data Centre and Fachinformationszentrum Karlsruhe Access Structures service www.ccdc.cam.ac.uk/structures.

[27] Z. Chen, C. S. Wannere, C. Corminboeuf, R. Puchta, P. von R. Schleyer, *Chem. Rev.* **2005**, *105*, 3842 – 3888.

[28] a) R. Herges, D. Geuenich, *J. Phys. Chem. A* **2001**, *105*, 3214 – 3220; b) D. Geuenich, K. Hess, F. Köhler, R. Herges, *Chem. Rev.* **2005**, *105*, 3758.

Manuscript received: August 30, 2020
Accepted manuscript online: January 6, 2021
Version of record online: March 5, 2021

